5-2020

# Optimization of RT-qPCR protocols to quantify chuA gene expression in Campylobacter jejuni mutants under iron-limited conditions

Jacob D. Wilbert
*University of Tennessee, Knoxville*, jacdwil1@vols.utk.edu

# Optimization of RT-qPCR protocols to quantify *chuA* gene expression in *Campylobacter jejuni* mutants under iron-limited conditions

Jacob Wilbert

Dr. Jeremiah Johnson M.S. Ph.D.

Department of Microbiology

University of Tennessee, Knoxville

## ABSTRACT

*Campylobacter jejuni* is the most prevalent cause of bacterial derived cases of gastroenteritis worldwide. Additionally, due to its severe symptoms and increasing antibiotic resistance, it is posing a serious threat to public health in most societies. *C. jejuni* warrants investigation in order to better understand the systems and mechanisms it utilizes to successfully infect humans and cause disease. The *chu* gene cluster is comprised of five genes employed in the uptake and utilization of heme as an iron source. These genes are regulated by two transcriptional regulators, Fur and HeuR, in an iron-dependent manner. Further investigation must be performed to fully understand how these two regulators work in tandem to regulate the *chu* system under differing iron conditions. Accordingly, this study reviews and refines the multifaceted protocols used prior to the quantitative analysis of *chuA* gene expression via Reverse Transcriptase-Quantitative Polymerase Chain Reaction (RT-qPCR). The topics addressed include bacterial growth conditions, RNA extraction, RNA purification, and primer optimization. The main implication of these optimized and refined protocols is a more efficacious approach to RT-qPCRs in future studies.

Keywords: *Campylobacter*, Fur, HeuR, *chu*, RT-qPCR

## BACKGROUND

*Campylobacter jejuni* is a motile, gram-negative bacteria and a worldwide threat to public health due to its severity of symptoms and rising antibiotic resistance **[9]**. Ninety-six million cases of diarrheal disease reported globally in 2010 were attributed to *Campylobacter* species with an estimated 1.3 million cases each year in the United States **[9]**. Of all of the bacterial causes of

gastroenteritis, *Campylobacter jejuni* is the most common in the United States (~45%), ahead of both *Salmonella* (~30%) and *E. coli* O157 (~5%) **[1]**. Common symptoms include fever, abdominal cramping, and bloody diarrhea while infants, elders, and people with underlying health problems are at increased risk for the more severe symptoms such as sepsis, Guillain-Barré syndrome, and death **[1]**.

Iron is a cofactor for many enzymes in processes such as the electron transport chain, which makes it a vital nutrient for bacterial infection **[2]**. *C. jejuni* cannot survive without iron, so it must have the ability to obtain it from the environment or its host organism. However, limitation of free iron is a common means of host nutritional immunity, so *C. jejuni* and most other pathogenic bacterial species have evolved various methods of iron acquisition **[2]**. They have developed the particular specialty of obtaining iron from the ubiquitous cofactor heme, as heme is the most abundant source of iron in humans. Because iron acquisition is critical, bacterial mechanisms of utilizing heme, and most iron sources, are very well refined and controlled **[2]**. Heme utilization is especially efficacious in tandem with the presence of blood in stool during campylobacteriosis.

One of these iron acquisition systems present in *C. jejuni* is the *chu* system. This is a system of five proteins that act in conjunction to uptake and utilize heme as an iron source **[8]**. The *chuA* gene encodes an extracellular heme receptor, *chuB* and *chuC* encode a permease and ATP binding domain, respectively, of a hemin ABC transporter, *chuD* encodes a hemin binding protein in the periplasm, and *chuZ* encodes a heme oxygenase that frees iron from heme **[8]**. *ChuZ* utilizes the same promoter region as *chuABCD,* but it is divergently transcribed **[8]**. Our unpublished data also shows the *chuABCD* system is transcribed as an operon, so *chuA* regulation should be representative of the system (Supplementary Figure S1).

In the presence of iron, the transcription of *chuZABCD* is repressed by the ferric uptake regulator (Fur) protein. Iron is an activating cofactor of the transcriptional regulator Fur, so as intracellular iron concentration increases, Fur is more active and binds to the promotor region of iron uptake genes, repressing transcription. The transcriptome of a *C. jejuni* 11168 wild type (WT) and Δ*fur* strain under iron-replete and iron-limited conditions was captured using RNAseq **[5]**. This revealed that, when compared to a WT strain under iron-replete conditions, the *chu* system is downregulated in WT under iron-limited conditions and upregulated in a Δ*fur* strain in iron-replete conditions. Additionally, under iron-limited conditions, there is no significant change in *chuA* expression between a WT strain and a Δ*fur* strain **[5]**.

Another transcriptional regulator, denoted HeuR (heme uptake regulator), has been shown to positively regulate the *chu* system, along with many other genes in *C. jejuni* 81-176. This regulatory mechanism is less well understood than Fur regulation, so further investigation must be done to understand HeuR regulation of the *chu* system **[8]**. It is known that HeuR also binds the *chuZA* promoter region and that each of the *chuABCD* genes is regulated similarly with the *chuZ* gene being less, but still significantly, affected. The same study also showed that with heme as the sole iron source both *heuR* and *chuA* mutant strains were significantly less viable when compared to the wild type strain with heme as an iron source **[8]**. Another study shows that *chuA* and *chuD* were very highly upregulated, >500 fold and >100 fold respectively, during human infection **[6]**. This fact suggests that the system is heavily utilized and may be necessary for *C. jejuni* to colonize the human gut. With increasing antibiotic resistance, finding novel treatments for campylobacteriosis warrants attention. If the *chu* genes are required for colonization, then they or other heme acquisition systems could potentially be targets for novel treatments.

Although the *chu* genes are shown to be downregulated both in a WT strain under iron-limited conditions and in a *heuR* mutant under iron-replete conditions, their differential expression has not yet been quantified in a *heuR* mutant under iron-limited conditions. Additionally, as Fur and HeuR both regulate the *chu* system at the same promoter, a study of differential expression needs to be performed in a *fur* + *heuR* double mutant strain to investigate the amount of *chu* expression without either of these transcriptional regulators **[5]**,**[8]**. Because *chuABCD* is transcribed as an operon, the expression of the system can be tentatively represented by *chuA* expression in Reverse Transcriptase Quantitative Polymerase Chain Reaction (RT-qPCR) (Supplementary Figure S1).

RT-qPCR is a method of quantifying gene expression based on the number of RNA transcripts present at a given time **[14]**. RNA is extracted from a sample and cDNA is synthesized from the RNA using reverse transcriptase. This cDNA is used as the starting template DNA in quantitative PCR with primers specific for a gene of interest and one or multiple internal control genes **[14]**. The qPCR mixture contains molecules that fluoresce when DNA is in a certain state, such as double stranded, that are read by the thermocycler every cycle. Every time the DNA replicates, each strand fluoresces, so as more DNA is synthesized fluorescence increases. The number of cycles that it takes to exceed a given amount of fluorescence is termed the Threshold Cycle ($C_T$) **[14]**.

The choice of internal control gene is vital to quantifying differential expression. Ideally, the best internal control genes will have no change in expression across many conditions, especially the experimental condition **[13]**. Sometimes referred to as “housekeeping genes” the best internal controls are very highly conserved between organisms and vital to survival. The expression of genes that encode proteins like RNA polymerases is rarely changed because the cell

is so reliant on their functionality, which is why they make perfect controls **[13]**. Because the expression of this gene does not change, the expression of the target gene can be quantified as expression is normalized to the internal controls. It is best to use more than one internal control to account for any possible failure to maintain unchanged expression in any one of the internal controls. This ensures that the change in the target gene's expression is being calculated accurately **[13]**.

The differential expression of the target gene is calculated by determining the change in $C_T$ values between the control and experimental conditions relative to the change in expression in the internal control between the conditions. This comparison can be performed using the $2^{-\Delta\Delta C_T}$ method, which was originally described by Livak and Schmittgen. This method will return the differential $C_T$ values as fold changes relative to the controls **[10]**.

**PURPOSE**

The aim of this study is to refine the protocols that precede the quantification of expression of the target gene through RT-qPCR in *C. jejuni* 81-176. Although the differential expression of the target gene *chuA* under conditions of interest will not be quantified in this study, I seek to establish the most consistent and effective protocols so that all subsequent studies aiming to use RT-qPCR are as efficient as possible. The immediate applications of this study will allow for the quantification of *chuA* expression in wild-type, *heuR* mutant, Δ*fur*, and Δ*fur* + *heuR*::kan double mutant strains in iron-limited conditions through the use of RT-qPCR. These protocols specific to *C. jejuni* may then be utilized for other genes and conditions of interest in future studies.

## BACTERIAL STRAINS AND GROWTH CONDITIONS

The strains of *Campylobacter jejuni* used in this study were 81-176 wild type, *heuR*::kan, Δ*fur*, and Δ*fur* + *heuR*::kan double mutant, with all mutants in a 81-176 background. Our *heuR*::kan mutant was created by inserting a kanamycin resistance cassette into the *heuR* gene to ultimately result in a nonfunctional protein, while the Δ*fur* mutant was a clean deletion. These four strains were routinely cultured on Mueller-Hinton (MH) agar supplemented with trimethoprim as a selection factor for *C. jejuni*, kanamycin when appropriate, and 5% sheep's blood for supplemental nutrients. All incubation periods were consistent at 37°C under microaerophilic conditions (85% $N_2$, 10 % $CO_2$, & 5% $O_2$).

In this study, control conditions are arbitrarily defined by the standard concentrations and species of iron contained in Mueller-Hinton (MH) broth. We have previously shown that deferoxamine mesylate (DFOM) at a total concentration of 1.5mM is effective at sequestering usable iron in liquid media and significantly reducing growth of *C. jejuni*. So, I define iron-limited conditions (the experimental condition) in this study as MH Broth with DFOM added to a final concentration of 1.5mM.

Cultures of each strain were inoculated on agar two days prior to the start of the experiment and grown overnight. Fresh lawns of each strain were spread on new agar using a disposable loop and grown overnight again. Cells were gathered using disposable loops and suspended in MH broth. Three sterile 250mL flasks were prepared with 100mL of sterile MH broth for each strain and each experimental condition (24 total). Each suspended strain was used to inoculate three flasks with standard iron concentrations and three flasks with limited iron concentrations to an initial $OD_{600}$ of 0.1.

In order to determine how long to grow the liquid cultures so that the RNA is captured mid-log in the growth phase, the absorbance at 600nm wavelength was measured each hour from hour 0 through hour 12, again at hour 16, then every 8 hours until 48 hours. The growth curves for the four strains in each condition are shown in Figure 1. It was determined from these growth curves that the bacterial growth is mid-log at approximately 6 hours ($OD_{600}$ = 0.2-0.25), so that is when the cultures will be captured for RNA extraction in future experiments.

**Figure 1** – Growth curves of 81-176 wild type, *heuR*::kan, Δ*fur*, and Δ*fur* + *heuR*::kan double mutant in **a)** standard and **b)** limited iron conditions. Time points were taken on the hour at time 0 through 12 hours, again after 4 hours, then every 8 hours until 48 hours. Time points were captured using absorbance at 600nm wavelength.

**a)**

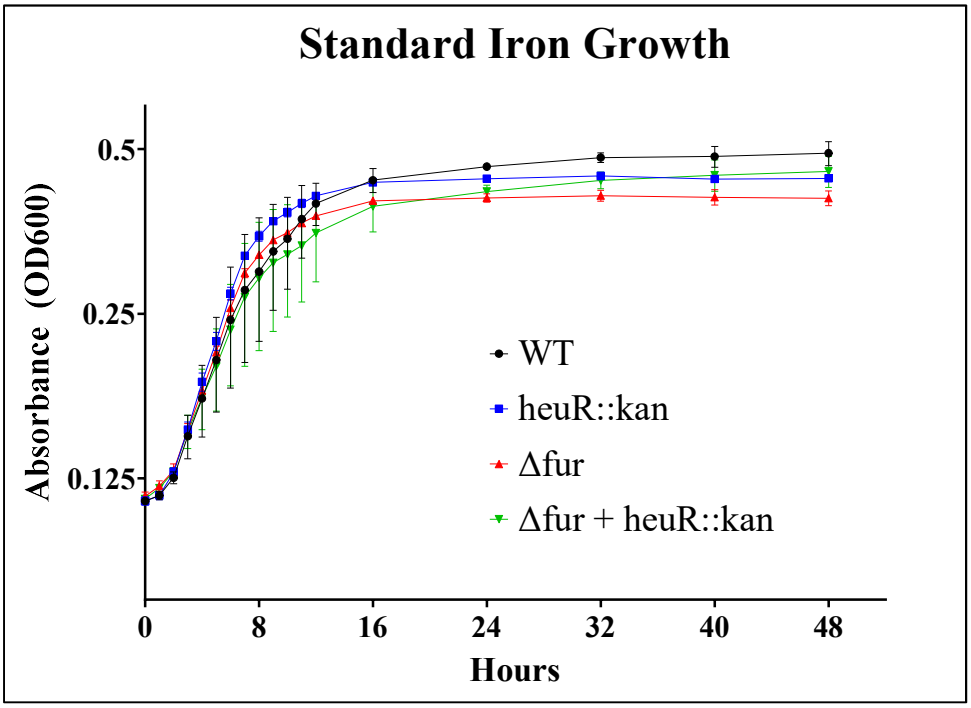


**b)**

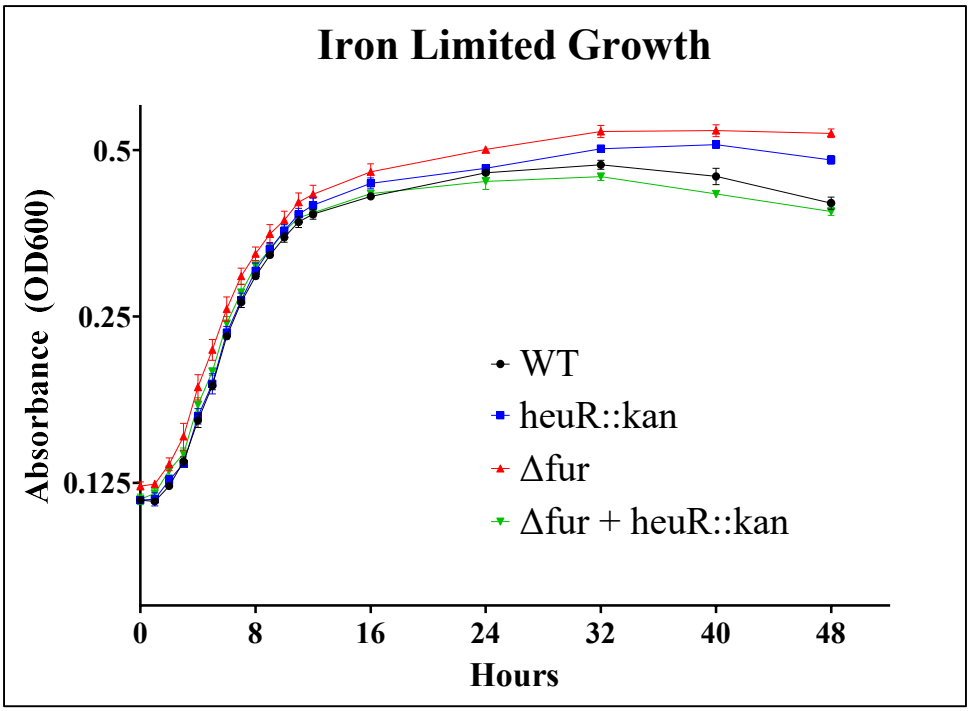

## RNA EXTRACTION

The process to extract RNA must be done with extreme caution as to not contaminate the samples with RNases. RNases are present on nearly every surface, as they are able to travel through air and are found plentifully in dust and on human skin **[11]**. Additionally, just as surfaces can be contaminated with RNases, all of the solutions and reagents used in this process can become contaminated easily. Consequently, it is critical that the following protocols are performed with fresh, nuclease-free reagents and equipment in a clean, ventilated hood. Nuclease-free disposable equipment such as filtered pipette tips will be designated as such, and non-disposable equipment such as pipettes and work surfaces should be cleaned with commercial RNase inhibitors prior to use.

RNA was extracted via phenol-chloroform extraction using RiboZol™ from VWR™. The extraction procedure was performed as follows:

1. Centrifuge the cell suspension to form a pellet and remove supernatant.
2. Resuspend the pellet in 500µL of RiboZol™.
3. Incubate for 5 minutes at room temperature to allow for complete lysis of cells.
4. Add 500µL of chloroform and vortex to mix. Incubate 2-3 minutes at room temperature. Chloroform should be handled in a chemical hood to avoid inhalation of vapors.
5. Centrifuge at 13,000 rpm for 15 minutes at 4°C.
6. Transfer clear aqueous phase to a new labeled microcentrifuge tube.
7. (Optional) Add 1µL of glycogen coprecipitant to help visualize RNA pellet.
8. Add 50µL of 7.5M Ammonium Acetate and 500µL of 100% Ethanol to each tube and incubate at -20°C for 2 hours.
9. Centrifuge at 12,000 x g for 15 minutes at 4°C.
10. Remove the supernatant and wash the pellet with 150µL of 70% ethanol.
11. Remove the supernatant and allow pellets and tubes to airdry for 20 minutes or until dry.
12. Resuspend the pellet in 25µL nuclease-free water and incubate samples for 10 minutes at 55-60°C to help dissolve the RNA pellet.
13. RNA can be used immediately or stored at -80°C.

Once the RNA is obtained, it must be analyzed to make sure it is usable. Firstly, the integrity of the samples should be assessed to confirm the absence of RNases. Then, the yield of RNA must be measured to ensure that there is enough sample RNA to use in downstream protocols. Lastly, the purity of the samples tested to detect any contaminants in the sample that may pose problems in subsequent reactions. The RNA samples obtained with this protocol had some contaminants, but they had decent yields (50-250ng/μL) and were considered intact. The following discussion will explain methods of analysis, how to remove contaminants from the samples, and ways to improve this protocol to prevent contamination.

There are multiple methods to analyze the integrity of the RNA extracted. The method that was used for this experiment was an agarose gel with added bleach to visualize total RNA. Intact RNA will appear as two bands in an agarose gel with the top band being approximately twice the intensity of the bottom band. The top band represents the large subunit rRNA, and the bottom band represents the small subunit rRNA. The bleach in the gel acts to inhibit any RNases that would otherwise be found in the gel that may degrade the RNA **[3]**. Alternatively, formaldehyde can be used to treat the gel, but this is more costly and requires more safety concerns. To make a bleach gel, the normal 1% agarose mixture is heated until the agarose is completely dissolved before pure bleach is added 1% v/v (1 mL beach into 99mL mixture) to the hot agarose mixture. The bleach can be added before the mixture is heated, but the bleach may vaporize and could cause harm to the user as it is being heated. Once the bleach is added and the mixture has cooled down, it can be poured into a mold with the addition of EtBr, and the gel can be used normally **[3]**. The integrity of the RNA samples extracted in this experiment are shown in Figure 2. There are two bands in all but one of the lanes with the top band being more intense than the bottom band, suggesting that the RNA in those samples is intact. The RNA samples in the lanes that do not show the same

banding patterns are likely to have been exposed to an RNase and the sample is degraded. Alternatively, the sample might not have had a high enough concentration of RNA to fluoresce visibly.

**Figure 2** – An image of RNA visualized by ethidium bromide in an agarose gel. In each of the first 12 lane on top and bottom, the top band shows the large subunit rRNA and the bottom band shows the small subunit rRNA. The RNA samples were loaded into the lanes as follows from left to right in triplicate: wild type, *heuR* mutant, Δ*fur*, Δ*fur* + *heuR* double mutant. Samples in the top lanes were from standard iron conditions, and the samples on the bottom lanes were from iron-limited conditions. DNA ladders were added in the rightmost visible lanes on top and bottom, and a positive gDNA control was added to the left of the ladder on the bottom.

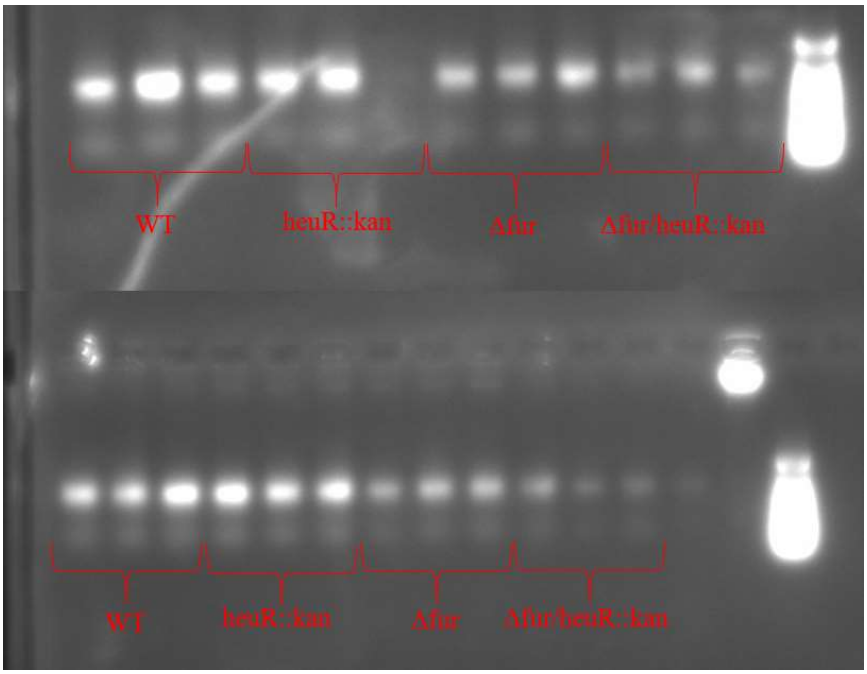


The RNA samples can be analyzed by spectrophotometry to find the yield and purity. The yield that is given, however, is not always reliable for two reasons. Firstly, all nucleic acids absorb at 260nm, so if there is any DNA contamination or free nucleotides then the concentration reading will be skewed. Secondly, if there is leftover phenolic and guanidine isothiocyanate reagents from the RNA extraction, they can absorb at and around 260nm and cause the concentration reading to be inaccurate **[7]**. A low yield can be increased by increasing the amount of cell suspension that is

pelleted, but the amount of RiboZol™ and other reagents should be increased incrementally as more cell suspension is used. To determine RNA purity, the 260/280 and 260/230 ratios must be determined. A pure RNA sample will have a 260/280 ratio of ~2.0 and a 260/230 ratio of ~2.0-2.2. If these ratios are lower than these expected values, then that means the RNA sample is not pure. Common contaminants can be phenol, proteins, and carbohydrates such as a glycogen coprecipitant **[7]**. The samples obtained in this experiment yielded concentrations between approximately 50 and 200 ng/μL and contained contaminants. Most of the 260/230 ratios were near or below 1.0 and the 260/280 ratios were near 1.5, indicating multiple species of contaminants.

It is important that these contaminants are not present in the RNA samples so that they do not disturb any downstream treatments such as the reverse transcription and qPCR. There are different ways to purify RNA samples, but some are more efficacious than others in that some methods result in a loss of RNA quantity. Using a commercial RNA cleanup kit is the easiest and quickest method to clean an RNA sample, but it can also result in a loss of RNA. Performing an additional phenol-chloroform extraction would remove protein and DNA contamination while sparing RNA quantity, but it could potentially introduce further phenol contamination if care is not taken. Ultimately, preserving a usable RNA concentration is of utmost concern, and after many trials of both methods, I have found that the best way to remove contaminants and preserve the RNA is to repeat phenol chloroform extractions. It is crucial to take great care and deliberation with every step as to not further contaminate the sample. It also seems that the most influential step in preventing contamination is the ethanol wash step. The RNA extraction protocol described previously utilized inadequate wash steps and, as a result, yielded highly contaminated samples. To increase the effectiveness of the ethanol wash steps, it should be performed with 1mL of 70%

ethanol and should be repeated at least once until all contaminants are removed. The added volume and steps will allow for greater solvation and removal of salt, protein, carbohydrate, phenol, and other contaminants, but with every time the wash step is performed, there is risk for losing RNA. If this protocol is adequately effective, then the initial phenol-chloroform extraction should be able to produce pure RNA with good yield and there should be no need for additional phenol-chloroform extractions. The revised protocol with additional wash steps is as follows:

1. Centrifuge the cell suspension to form a pellet and remove the supernatant.
2. Resuspend the pellet in 500µL of RiboZol™.
3. Incubate for 5 minutes at room temperature to allow for complete lysis of cells.
4. Add 500µL of chloroform and vortex to mix. Incubate 2-3 minutes at room temperature. Chloroform should be handled in a chemical hood to avoid inhalation of vapors.
5. Centrifuge at 13,000 rpm for 15 minutes at 4°C.
6. Transfer clear aqueous phase to a new labeled microcentrifuge tube.
7. (Optional) Add 1µL of glycogen coprecipitant to help visualize RNA pellet.
8. Add 50µL of 7.5M Ammonium Acetate and 500µL of 100% Ethanol to each tube and incubate at -20°C for 2 hours.
9. Centrifuge at 12,000 x g for 15 minutes at 4°C.
10. Remove the supernatant and wash the pellet with 1mL of 70% ethanol.
11. Repeat wash step at least once to ensure thorough removal of contaminants.
12. Remove the supernatant and allow pellets and tubes to airdry for 20 minutes or until dry.
13. Resuspend the pellet in 25µL nuclease-free water and incubate samples for 10 minutes at 55-60°C to help dissolve the RNA pellet.
14. RNA can be used immediately or stored at -80°C.

**RNA PURIFICATION**

It is critical that there is no detectable genomic DNA contamination in an RNA sample if it is to be used in RT-qPCR. When RNA is reverse transcribed, the amount of cDNA generated reflects the proportion of target mRNA transcripts and, in turn, the amount that the gene of interest was expressed. If there is existing gDNA in the sample, then the primers intended to bind and

amplify the cDNA will bind the gDNA and amplify it as well. This will result in an uncontrolled overestimation of target gene expression. To test whether there is gDNA contamination in the sample, a standard PCR can be run with the sample and a primer set for a positive control gene, *mapA* in this case, and the product can be analyzed via gel electrophoresis. The PCR should be run for 40 cycles, the same as qPCR, because the difference in DNA amplification between 30 and 40 cycles is one thousand-fold, so this will reveal absolutely any gDNA that would also be revealed in qPCR. The RNA samples I obtained were tested for gDNA in the following way:

- 25µL total reaction volume
  - 12.5µL Thermo Fisher DreamTaq DNA polymerase
  - 9.5µL nuclease-free water
  - 1µL [10mM] *mapA* forward primer
  - 1µL [10mM] *mapA* reverse primer
  - 1µL RNA sample
- 95°C initial denature for 3 minutes
- 95°C denature for 30 seconds, x40 cycles
- 45°C annealing stage for 30 seconds, x40 cycles
- 65°C elongation stage for 1 minute, x40 cycles
- 65°C final elongation for 7 minutes

The PCR products obtained from this reaction were analyzed via gel electrophoresis on a 1% agarose gel. The PCR revealed that there was significant gDNA contamination in all 24 RNA samples, as shown in Figure 3. The presence of these bands indicates that there is preexisting template DNA in the RNA samples and that our positive control gene, *mapA,* was able to amplify. Our primers for *mapA* generate an amplicon that is 500 base pairs in size. If these samples were used in qPCR as they are, all of this gDNA would amplify on top of the target cDNA and cause the $C_T$ values to be inaccurate.

**Figure 3** – An image of genomic DNA contamination in RNA samples prior to any DNase treatments. Genomic DNA was amplified by PCR and visualized by ethidium bromide on an agarose gel. The visible band represents the positive

control gene *mapA*. RNA samples are arranged as follows from left to right in triplicates: wild type with standard iron, *heuR*::kan mutant with standard iron, Δ*fur* with standard iron, Δ*fur* + *heuR*::kan double mutant with standard iron, wild type with limited iron, *heuR*::kan mutant with limited iron, Δ*fur* with limited iron, and Δ*fur* + *heuR*::kan double mutant with limited iron.

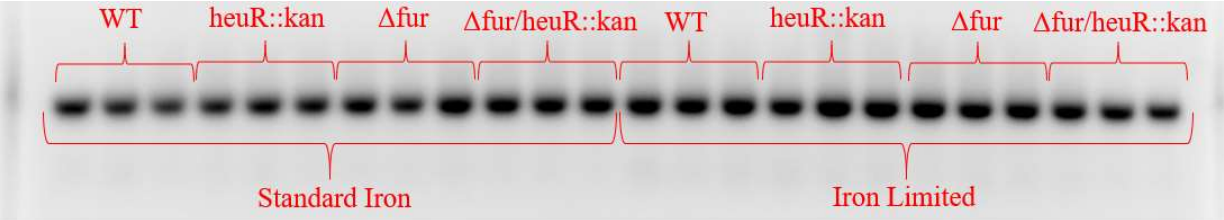


To remove contaminating genomic DNA from these RNA samples, a DNase treatment must be performed. The DNase is from an Ambion® DNase I kit. The manufacturer's recommendation for use of this product is adding the DNase buffer (10X) to a concentration of 1X in the RNA sample, adding 1µL of DNase enzyme (2U), and incubating the reaction at 37°C for 30 minutes. This reaction should digest up to 2µg of DNA, but after four subsequent iterations of this reaction on the same samples, there was still genomic DNA contamination. There is not an inherent problem with having to do multiple DNase treatments; however, after every treatment a step is required to either inactivate or remove the DNase enzyme from the reaction. There are a few manufacturer-recommended methods of inactivating or removing the DNase, but each poses its own challenges.

The first method is by phenol chloroform extraction, which may introduce a number of contaminants back into the sample or lose RNA during any one of the steps. Another method is by heat inactivation. The manufacturer recommends adding EDTA to 5mM and heating to 75°C for 10 minutes to inactivate the DNase. The problem with this method is that EDTA is a magnesium chelator. If too much EDTA accumulates from subsequent reactions it will inhibit downstream PCRs because magnesium is essential for enzyme function. Additionally, if more than one DNase treatment is needed, then any extra EDTA might inactivate any new DNase. A third manufacturer-recommended method is through gel purification where samples may be run through an agarose

gel to separate the components of the reaction, but this method results in the loss of RNA through the gel extraction. A final method, one that was not mentioned by the manufacturer, is to run the reaction mixture through an RNA cleanup kit. Some of these kits are designed to do DNase treatments in-column, so they are effective at removing the reaction components and returning only the RNA. The only challenge with these is that they often lose RNA quantity. The challenge presented here is to minimize the number of times the sample has to be treated because the more times it has to be treated, the more times it has to be cleaned, meaning the DNase treatment must be optimized to work at maximum capacity.

The DNase treatment was optimized by manipulating the amounts of enzyme and the buffer concentration. According to the product description, Ambion® DNase I is most effective when the concentration of magnesium is 5mM, yet when the buffer is added to a final 1X concentration, magnesium is only at a concentration of 2.5mM. So, the treatment at 1X buffer concentration was compared to a treatment at 2X buffer concentration. Additionally, increasing the amount of enzyme in the reaction should increase its capacity, so the amount of enzyme was manipulated in conjunction with both buffer conditions. In total, there were four reaction combinations: 1X buffer and 1µL enzyme, 2X buffer and 1µL enzyme, 1X buffer and 2µL enzyme, and 2X buffer and 2µL enzyme. All four of these reactions received 1µL of the same untreated RNA sample and nuclease-free water up to a total volume of 20µL, and they were all treated simultaneously in the same heating block at 37°C for 30 minutes. A Zymo Research RNA Clean & Concentrator™ kit was used to clean the reactions and then the product was amplified using PCR as described above. Figure 4 shows the results of these four reactions. All of the treatments were successful in removing gDNA, but the reaction with the doubled enzyme amount and 2X buffer concentration was clearly the most effective. There is still some gDNA contamination visible, but in this small

amount it would not noticeably affect a qPCR. Regardless, more optimization was performed to ensure there is absolutely no traceable amount of gDNA.

**Figure 4** – An image of DNase treatments after being cleaned with a Zymo Research RNA Clean & Concentrator™ kit and remaining gDNA amplified by a 40 cycle PCR. The reactions are ordered in the lanes from left to right as follows: 1) 1X buffer and 1µL enzyme, 2) 2X buffer and 1µL enzyme, 3) 1X buffer and 2µL enzyme, 4) 2X buffer and 2µL enzyme, 5) a sample of the same untreated RNA that went into each of the DNase treatments, and 6) a gDNA positive control.

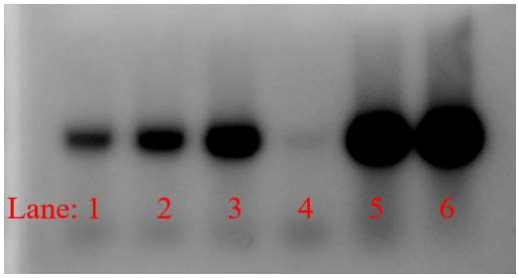


To simulate performing two DNase treatments while only having to clean one time, the reactions were spiked with additional amounts of reagents. In total, there were three different reactions. All three started with 2µL of enzyme, 2X buffer concentration (4µL), 1µL untreated RNA sample, and nuclease-free water up to 20µL and were treated for 30 minutes at 37°C. Subsequently, they were all spiked with an extra 2µL of enzyme, one was also spiked with 4µL of buffer, the second was also spiked with 2µL of buffer, and the third did not receive extra buffer. They were treated again for 30 minutes at 37°C, then cleaned and amplified as previously described. Figure 5 shows the results of this optimization. The reaction that was spiked with 2µL of DNase and an additional 4µL of buffer performed the best and was capable of digesting all traces of gDNA. This method effectively performs two DNase treatments with the most effective combination of reagents while only having to clean the reaction once. This allows for the complete removal of contaminating gDNA while preserving as much RNA in the sample as possible.

**Figure 5** – An image of DNase treatments after being spiked with varying additional reagents. In the lanes from left to right: 1) a DNA ladder, 2) a DNase treatment that was spiked only with 2µL of DNase, 3) a DNase treatment that was spiked with 2µL of DNase and 2µL of buffer, 4) a DNase treatment that was spiked with 2µL of DNase and 4µL of buffer, 5) the untreated RNA that went into each reaction, and 6) a gDNA positive control.

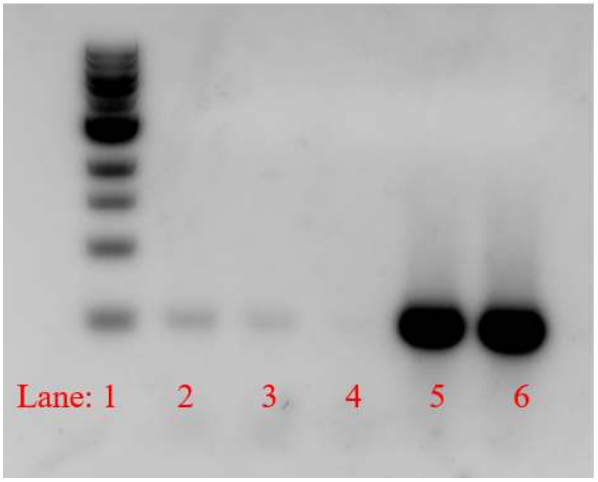


Once all of the contaminating gDNA is removed from the samples, the RNA should be tested again for integrity. This can be done using commercial methods like an Agilent Technologies, Inc. Bioanalyzer kit or with a bleach gel **[3]**. Using the commercial method is preferred, as it is more accurate and detailed. After the quality of the RNA is established as intact, then it is ready to be used for RT-qPCR.

## RT-qPCR PRIMER DESIGN AND OPTIMIZATION

New qPCR primers were designed for the *chuA* gene using NCBI Primer BLAST® and analyzed and synthesized by Integrated DNA Technologies™. I obtained primer sequences for an internal control, *rpoA*, from a publication by Ritz et al. which were also analyzed and synthesized by Integrated DNA Technologies™ **[13]**. The primer set for *chuA* was designed to be as similar to *rpoA* as possible to allow for maximum efficiency from both primers when used together under the same parameters. The properties of the primers are shown in Table 1.

**Table 1 –** A listing of qPCR primers used in this study and their properties.

| Primer | Nucleotide sequence (5'-3') | $T_m$ (°C) | %GC |
|---|---|---|---|
| *chuA* forward | ACC AGC AGT GGC TAT CTA AC | 61.4 | 50 |
| *chuA* reverse | CAG GGC GAT TGA TTT GTG TG | 61.4 | 50 |
| *rpoA* forward | CGA GCT TGC TTT GAT GAG TG | 61.3 | 50 |
| *rpoA* reverse | AGT TCC CAC AGG AAA ACC TA | 60.9 | 45 |

Several tests of optimization must be conducted to ensure the primer sets perform at their optimal efficiency. The ideal efficiency (100% amplification) of a qPCR reaction is when the amount of template DNA increases two-fold with each reaction cycle **[4]**. If a primer set is inefficient then not all of the DNA will be replicated in any single reaction which will result in an underestimation of the amount of initial template DNA. Several factors that can lead to inefficient primers are annealing temperatures being too high, primer concentrations being too low, or primer GC content being too low. If a primer set results in greater than 100% amplification, that is indicative of nonspecific binding or primer secondary structures. The polymerase mixture used in these reactions is iTaq™ Universal SYBR™ Green Supermix from Bio-Rad Laboratories, Inc. Because SYBR™ Green fluoresces when DNA is double stranded, primer dimers, secondary primer structures such as hairpins, and primers binding nonspecifically to DNA all will fluoresce and be measured as replicated DNA. These occasions will result in an overestimation of the amount of initial template DNA.

In order to find the best annealing/elongation temperature parameter to use in the experimental qPCR, the primers must first be tested at many different temperatures. I performed a sample qPCR with a gradient of annealing/elongation temperatures and the following parameters in duplicate for both primer sets:

- 20µL reaction volume
    - 10 µL iTaq™ Universal SYBR™ Green Supermix
    - 7 µL nuclease free water
    - 1 µL forward primer (10µM stock; 500nM final concentration)
    - 1 µL reverse primer (10µM stock; 500nM final concentration)
    - 1 µL gDNA at 10ng/µL concentration
- 95°C Initial denature, 3 minutes
- 95°C denature, 30 seconds, x40 cycles
- Annealing/elongation temperature within 56-64°C, 1 minute, x40 cycles
- Duplicate reactions for each primer set, for each of the 8 gradient temperatures for a total of 32 reactions.

The quality of each primer set can be assessed first by calculating the range of the $C_T$ values measured from the range of temperatures. A well-designed primer will have little change in $C_T$ value over a range of temperatures, indicating a binding affinity that is independent from temperature conditions **[4]**. This is important when working with multiple primer sets as it is possible that each one will have different optimal conditions. If one primer set anneals best at 55°C and another at 65°C, then your reaction will be less than optimal for one or both of the primer sets. However, if one or both primer sets are able to anneal with high efficiency over a wide range of temperatures, then having to use a temperature that accounts for different primer sets does not become problematic. The optimal annealing temperature for each primer in this test was determined by finding the lowest $C_T$ value, which indicates the highest amount of amplification.

As Table 2 depicts, there is high variability in the range and average of $C_T$ values of the technical replicates of each primer set. Despite this variability between replicates the different primer sets are still comparable, which may indicate that the variability is due to systematic error in the reaction setup. Both primer sets were able to produce an appreciably low range in $C_T$ values and had comparable average $C_T$ values, meaning that these primer sets are relatively independent

of changing annealing temperatures and amplify DNA at similar efficiencies. When taking both replicates into account and regardless of error, it seems the optimal annealing/elongation temperature to use for these primer sets is approximately 62°C.

**Table 2** – Threshold cycle ($C_T$) values for *chuA* and *rpoA* primer sets for a range of annealing/elongation temperatures. Bolded values mark the lowest $C_T$ value for each replicate range of temperatures.

| Annealing/Elongation Temperature | *chuA* | | *rpoA* | |
|---|---|---|---|---|
| 64°C | 15.56 | 18.77 | 15.04 | 18.51 |
| 63.6°C | 15.33 | 17.07 | **14.73** | 19.02 |
| 62.7°C | 14.84 | **15.81** | 14.83 | **15.39** |
| 61.1°C | 15.12 | 16.85 | 15.20 | 16.06 |
| 59.2°C | **14.47** | 27.86 | 15.17 | 35.01 |
| 57.6°C | 14.66 | 22.18 | 15.53 | 35.15 |
| 56.5°C | 16.02 | 21.70 | 15.15 | 32.46 |
| 56°C | 16.74 | 36.62 | 16.29 | N/A |
| Average | 15.34 | 22.11 | 15.24 | 24.51 |
| Range | 2.27 | 20.81 | 1.56 | 19.76 |

Another parameter of a qPCR that must be optimized is the concentration of primers used in each reaction. The optimal primer concentration will vary based on the properties of the primers themselves. Primers that have a weaker binding affinity to their gene might need a higher concentration to maintain the optimum efficiency of replication. If there is not enough primer or the primer is too weak, then the reaction could be inefficient. To optimize the concentrations of each primer, all other parameters were held constant as they were in the temperature gradient test, except for temperature which was held at 62°C. Primer concentration was increased stepwise from 200nM to 500nM in duplicate reactions of each primer pair. Results from this test are shown in Table 3.

Assuming that a lower $C_T$ value represents a higher reaction efficiency, there was no considerable difference in reaction efficiency between primer concentrations of 300nM and 500nM. The reactions for *rpoA* at 400nM primer concentration yielded no results, which was likely due to an error in the reaction setup that resulted in each replicate missing a reaction component. However, because of the lack of change in efficiency between these values, it is also likely that 400nM would have similar efficiency. Additional experimentation would be needed to show that, and further reactions will not be based on a primer concentration of 400nM because of this lack of confirmation. Based on this test and preexisting standard practices, further experiments will be conducted with a primer concentration of 500nM.

**Table 3** – Threshold cycle ($C_T$) values for *chuA* and *rpoA* primer sets at various primer concentrations. Bolded values mark the lowest $C_T$ value for each replicate range of primer concentrations.

| Primer Concentration (nM) | *chuA* | | *rpoA* | |
|---|---|---|---|---|
| 200 | 12.13 | 11.88 | 12.18 | 11.91 |
| 300 | **11.73** | 11.68 | **11.55** | 11.69 |
| 400 | 11.86 | **11.65** | N/A | N/A |
| 500 | 11.74 | 11.9 | 11.64 | **11.49** |

After these tests of optimization are complete, the primer efficiencies must be tested. This can be done by making reactions with serial dilutions of template DNA, typically ten-fold, and plotting their $C_T$ values against the number of dilutions to create a standard curve **[4]**. If a primer set is 100% efficient, the $C_T$ values will increase as the amount of starting template DNA decreases with a negative slope. The slope corresponds with the number of cycles that it takes to amplify the same amount of template DNA that is changed by each dilution. So, if the reactions have ten-fold changes in starting template, then you would expect to see a slope of -3.322 because it takes 3.322 cycles to generate a ten-fold increase in DNA at 100% efficiency **[4]**. However, if the $C_T$ values

change with a lesser or greater magnitude of slope, that indicates that the primers are over or under 100% efficient, respectively. For example, if your primers are 150% efficient then you would expect a lower slope because it takes less cycles to achieve ten-fold amplification. Likewise, if your efficiency is 50%, then you would expect a higher slope because it takes more cycles to achieve the same ten-fold change in DNA. Assuming 100% efficiency, the relationship between the dilution factor, *D*, and the number of cycles, *n*, it takes to amplify that amount of DNA is shown below as (1). You can find the theoretical slope by solving for *n*, which is shown below by (2) **[4]**.

$$D = 2^n \tag{1}$$

$$n = \log_2(D) \tag{2}$$

To find the actual efficiency of the primer set, you much plot each $C_T$ value against its fold change and find the slope of the line. Efficiency (*E*) can then be calculated with (3) and percent efficiency (*%E*) can be calculated with (4).

$$E = D^{-1/\text{slope}} \tag{3}$$

$$\%E = (E\text{-}1) * 100\% \tag{4}$$

The obtained $C_T$ values and efficiencies for the *chuA* and *rpoA* primer sets are displayed in Table 4, and the $C_T$ values are plotted in Figure 6. In this case, a dilution factor of 5 was used across 4 reactions in duplicate for each primer set, meaning the first reaction had a set amount of template, then each subsequent reaction had 5 times less template than the previous.

Based on the standard curve, both the *chuA* and *rpoA* primer sets work beyond maximum efficiency. This suggests that there is some extraneous double stranded binding, whether that is primer dimers, primer secondary structures, or nonspecific primer binding. After analyzing the

melt curve of both primer sets, there is only one peak very consistently at 75-76°C which implies that there is no significant alternative double stranded DNA formation. It is possible that the higher efficiency is due to errors in preparing the reactions. Ideally, these primers should be redesigned to be closer to 100% efficiency. However, these primers could be used, and the qPCR results could be analyzed with the Pfaffl method, which accounts for different reaction efficiencies, instead of the $2^{-\Delta\Delta C_T}$ method **[12]**.

**Table 4** – Threshold cycle ($C_T$) values of *chuA* and *rpoA* at varying fold changes of starting template DNA. Efficiency (E) and percent efficiency (%E) were calculated from the slopes of each replicate.

| Starting Template DNA (ng) | *chuA* | | *rpoA* | |
|---|---|---|---|---|
| 2 | 15.35 | 15.52 | 15.08 | 15.18 |
| 10 | 13.21 | 13.08 | 12.85 | 12.96 |
| 50 | 11.35 | 11.1 | 11.12 | 11.08 |
| 250 | 10.2 | 9.73 | 9.8 | 9.69 |
| | | | | |
| Slope | -1.731 | -1.935 | -1.757 | -1.835 |
| E | 2.53 | 2.3 | 2.5 | 2.4 |
| %E | 153% | 130% | 150% | 140% |

**Figure 6** – Standard curves of **a)** *chuA* and **b)** *rpoA* primer sets. Duplicate reactions are overlaid on each graph. The equation of each replicate is labelled in standard slope-intercept form. Starting template DNA refers to the initial amount of DNA added to each reaction, and each step is a five-fold increase in the amount.

**a)**

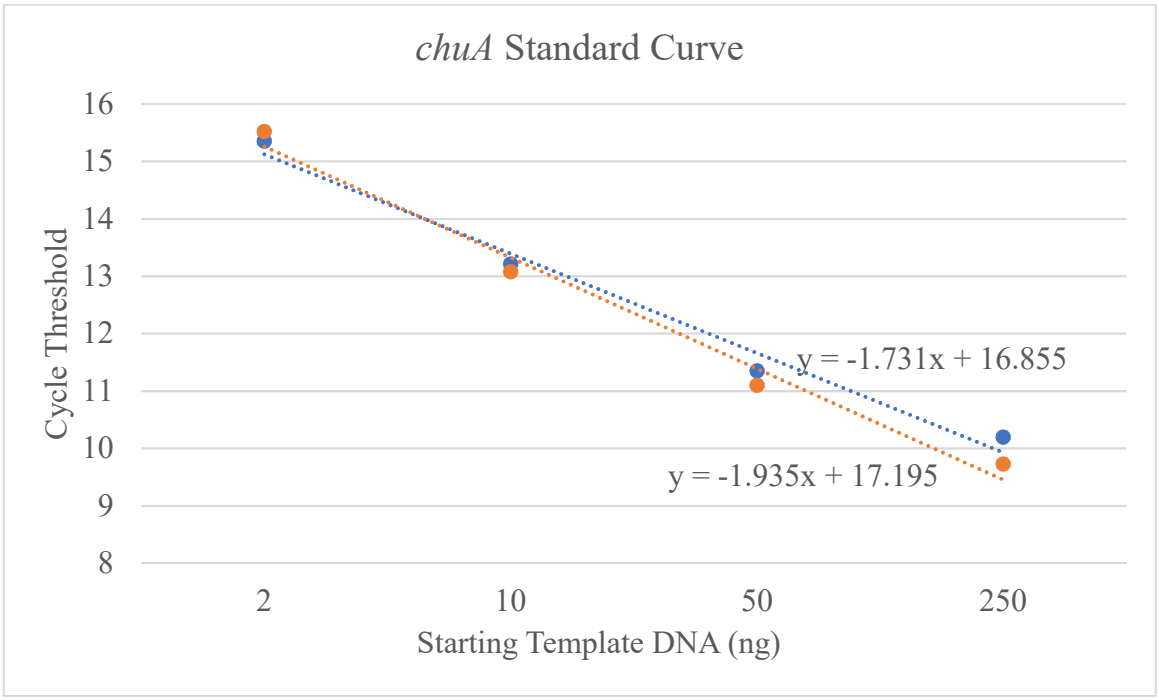


**b)**

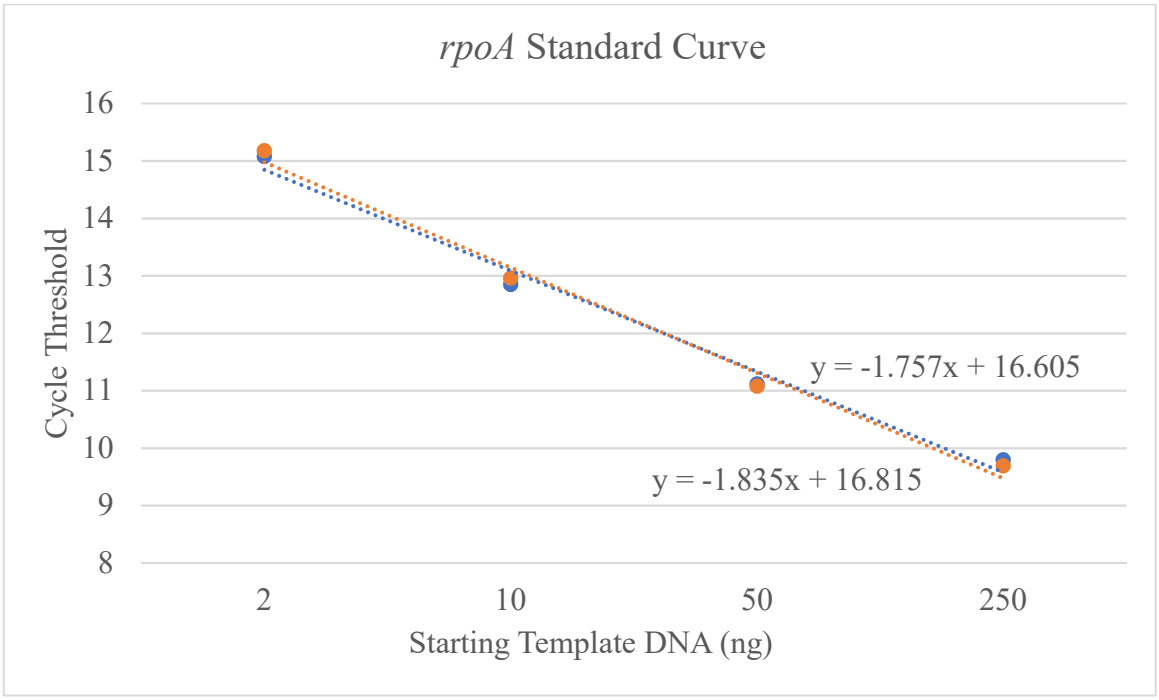

## IMPLICATIONS AND CONCLUSIONS

The aim of this study was to refine the protocols that precede the quantification of expression of the target gene through RT-qPCR in *C. jejuni* 81-176. If the methods developed and refined here are successful, these preparations can be used to attain pure, intact RNA and to optimize primer sets. Once pure, intact RNA is obtained and the primer sets are optimized, the next step is to generate cDNA and to quantify the target gene. Because, pure RNA from this experiment has yet to be obtained, this step has not been optimized. Further experimentation with this reaction is necessary to determine the amounts of reagent to add and reaction times. It is probable that, similar to the DNase treatments, adding more enzyme and buffer will increase the effectiveness of the reaction. Additionally, testing longer reaction times might yield better results.

If Fur and HeuR control the *chu* system how we expect, then we would expect to see increased expression of *chuA* in the *fur* mutant and decreased expression in the *heuR* mutant when compared to the WT strain in similar conditions. As iron is an activating cofactor of Fur, we would expect to see higher *chuA* expression in general under iron-limited conditions compared to standard iron conditions. Physiologically, this makes sense because as the presence of iron decreases in the cell, heme uptake should increase to replenish the intracellular iron concentration. However, it is difficult to speculate specific levels of expression in confounding conditions, such as a mutant strain under iron-limited conditions. The level of expression is difficult to attribute to any one of these factors under iron-limited conditions without actually performing the experiment and comparing it to its corresponding control.

Further, as both of these regulators use the same promoter for the *chu* genes, this investigation might provide insight into how they interact with each other. In the Δ*fur* + *heuR*::kan double mutant, neither transcriptional regulator is present. So, unless there is another regulator

acting on this promoter, the basal rate of expression should be detected in both the presence and absence of iron. I propose that without these regulators there is no sensory mechanism to regulate expression of the *chu* genes, so similar levels of expression should be observed with and without iron. When looking at this basal rate in comparison to the level of expression in a single mutant strain and wild type in both conditions, it could reveal how the presence or absence of either regulator affects the other. For example, the repressor is absent in a Δ*fur* strain, so expression increases. Not only is the repressor absent, but the activator is now able to bind to the promoter because there is no longer binding competition for the promoter. This aspect of *chu* control needs further investigation to determine the mechanisms of competition between Fur and HeuR regulation.

## LITERATURE REFERENCED


**[1]** Altekruse, S. F., Stern, N. J., Fields, P. I., and Swerdlow, D. L. (1999). Campylobacter jejuni—An Emerging Foodborne Pathogen. *Emerg. Infect. Dis.* 5, 28–35. doi:10.3201/eid0501.990104.

**[2]** Anzaldi, L. L., and Skaar, E. P. (2010). Overcoming the Heme Paradox: Heme Toxicity and Tolerance in Bacterial Pathogens. *IAI* 78, 4977–4989. doi:10.1128/IAI.00613-10.

**[3]** Aranda, P. S., LaJoie, D. M., and Jorcyk, C. L. (2012). Bleach gel: A simple agarose gel for analyzing RNA quality. *ELECTROPHORESIS* 33, 366–369. doi:10.1002/elps.201100335.

**[4]** Bustin, S., and Huggett, J. (2017). qPCR primer design revisited. *Biomolecular Detection and Quantification* 14, 19–28. doi:10.1016/j.bdq.2017.11.001.

**[5]** Butcher, J., Handley, R. A., van Vliet, A. H. M., and Stintzi, A. (2015). Refined analysis of the Campylobacter jejuni iron-dependent/independent Fur- and PerR-transcriptomes. *BMC Genomics* 16, 498. doi:10.1186/s12864-015-1661-7.

**[6]** Crofts, A. A., Poly, F. M., Ewing, C. P., Kuroiwa, J. M., Rimmer, J. E., Harro, C., et al. (2018). Campylobacter jejuni transcriptional and genetic adaptation during human infection. *Nat Microbiol* 3, 494–502. doi:10.1038/s41564-018-0133-7.

**[7]** Desjardins, P., and Conklin, D. (2010). NanoDrop Microvolume Quantitation of Nucleic Acids. *JoVE*, 2565. doi:10.3791/2565.

**[8]** Johnson, J. G., Gaddy, J. A., and DiRita, V. J. (2016). The PAS Domain-Containing Protein HeuR Regulates Heme Uptake in *Campylobacter jejuni*. *mBio* 7, e01691-16, /mbio/7/6/e01691-16.atom. doi:10.1128/mBio.01691-16.

**[9]** Laughlin, M. E., Chatham-Stephens, K., and Geissler, A. L. (2019). Campylobacteriosis. *Travelers' Health*. Available at: https://wwwnc.cdc.gov/travel/yellowbook/2020/travel-related-infectious-diseases/campylobacteriosis.

**[10]** Livak, K. J., and Schmittgen, T. D. (2001). Analysis of Relative Gene Expression Data Using Real-Time Quantitative PCR and the 2−ΔΔCT Method. *Methods* 25, 402–408. doi:10.1006/meth.2001.1262.

**[11]** New England BioLabs, Inc. Avoiding Ribonuclease Contamination. *New England BioLabs®, Inc.* Available at: https://www.neb.com/tools-and-resources/usage-guidelines/avoiding-ribonuclease-contamination [Accessed April 17, 2020].

**[12]** Pfaffl, M. W. (2001). A new mathematical model for relative quantification in real-time RT-PCR. *Nucleic Acids Research* 29, 45e–445. doi:10.1093/nar/29.9.e45.

**[13]** Ritz, M., Garenaux, A., Berge, M., and Federighi, M. (2009). Determination of rpoA as the most suitable internal control to study stress response in C. jejuni by RT-qPCR and application to oxidative stress. *Journal of Microbiological Methods* 76, 196–200. doi:10.1016/j.mimet.2008.10.014.

**[14]** Singh, J., Birbian, N., Sinha, S., and Goswami, A. (2014). A critical review on PCR, its types and applications. *International Journal of Advanced Research in Biological Sciences* 1, 65–80.

**PRODUCTS AND SERVICES REFERENED**

RiboZol™ by VWR™
https://us.vwr.com/store/product/7437721/vwr-life-science-ribozoltm-rna-extraction-reagent

Ambion® nuclease-free Dnase I
https://www.thermofisher.com/order/catalog/product/AM2224#/AM2224

RNA Clean & Concentrator™ by Zymo Research
https://www.zymoresearch.com/collections/rna-clean-concentrator-kits-rcc/products/rna-clean-concentrator-5

Bioanalyzer RNA kit by Agilent Technologies, Inc.
https://www.agilent.com/en/product/automated-electrophoresis/bioanalyzer-systems/bioanalyzer-rna-kits-reagents

National Center for Biotechnology Information (NCBI) Primer-BLAST®
https://www.ncbi.nlm.nih.gov/tools/primer-blast/

qPCR primers synthesized by Integrated DNA Technologies™
https://www.idtdna.com/pages

iTaq™ Universal SYBR™ Green Supermix by Bio-Rad Laboratories, Inc.
https://www.bio-rad.com/en-us/product/itaq-universal-sybr-green-supermix?ID=M87FTF8UU

## SUPPLEMENTARY FIGURES

**Figure S1 –** An image of intergenic sequences showing amplicons that indicate shared transcription between the *chuABCD* genes. From left to right: a 1 kilobase DNA ladder, cDNA of *chuAB* intergenic region, RNA of *chuAB* intergenic region prior to reverse transcription, cDNA of *chuBC* intergenic region, RNA of *chuBC* intergenic region prior to reverse transcription, cDNA of *chuCD* intergenic region, RNA of *chuCD* intergenic region prior to reverse transcription.